

Sliding Mode Controller for Pressure Regulation in PEM Fuel Cell

E.A.MohamedAli¹

National College of Engineering
Tirunelveli, Tamilnadu, India
ea_mdali2003@yahoo.co.in

A.Abudhahir²

Veltech Multi Tech Dr.Rangarajan, Dr.Sakunthala Engineering College
Chennai, Tamilnadu, India
abudhahir74@yahoo.co.in

A.ManivannaBoopathi³

Bahrain Training Institute
Isa Town, Bahrain
arumugamboopathy@gmail.com

Abstract—The regulation of reactants pressure and supply are prerequisite for the performance and prolong life of Proton Exchange Membrane Fuel Cell (PEMFC). The depleted supply of reactants may deteriorate the operation of PEMFC. Moreover, the large deviation of reactants pressure can cause severe damage to the stack. The main aim of this paper is to control the pressure of hydrogen at anode and oxygen at cathode side by maintaining hydrogen and oxygen flow rates at optimum levels during dynamic load conditions. Sliding Mode Controller (SMC) is employed to control the reactants pressure at set point under dynamic load change. The results reveal that SMC employed in PEMFC produce better response than the PI controller reported earlier.

Keywords—PEMFC, Pressure regulation, Hydrogen Flow Rate, Oxygen Flow Rate, SMC.

I.INTRODUCTION

A fuel cell is an electrochemical energy converter which produces clean and green electricity from chemical energy of the hydrogen without undergoing combustion process. The electrochemical reaction of fuel cell discharges water and heat as byproducts. In comparison with other types of fuel cells, PEMFC has charming features like compact size, light weight, high power and current densities, low operating temperature, quick startup and zero emission. Due to its attractive features, PEMFC will become suitable energy converter for automotive, stationary and portable application in near future. The cost and durability of PEMFC restricts the commercialization and wide publicity of the product.^[1] Thus the proper selection of controller for maintaining the parameters ensures the performance and longevity of the cell.^[2]

Many control strategies addressed in literature to retain oxygen stoichiometric ratio for shunning oxygen starvation, ranging from feed forward control,^{[3],[4]} LQR control,^{[5]-[7]} Fuzzy logic control,^{[8],[9]} Neural network control,^{[10],[11]} Parameter optimized feed forward fuzzy logic control with feedback PID control^[12] and Model predictive control.^{[13],[14]} However, the performance and

longevity of PEMFC are mainly concerned with the proper control of the reactant pressure on both side of the electrodes.^[15] It is obvious that cell voltage, overall cell efficiency, energy density are increased and also the amount of reactant humidification requirements reduced along with increase in partial pressure of Hydrogen and Oxygen. But on the contrary the power required for compressor to supply Oxygen is increased.^[16] Hence, the optimum reactant gases are supplied to the PEMFC is 3 to 5atm. It is evident that the reactants' supply must always meet the dynamic load demand of PEMFC, since the current drawn for the cell is directly depended on the amount of Hydrogen and Oxygen supply. This change in concentration of the reactants will immediately cause a reduction in the partial pressure of the reactants. The large deviation in pressure difference between the reactants on both sides can cause severe damage to the membrane. Hence, the pressure difference must always be kept below 0.5atm to protect the membrane from the risk of severe damage.^[2]

The main objective of this work is to keep the partial pressure of the reactants at the desired level in order to avoid the detrimental degradation of the life of PEMFC and also hold the pressure difference between the hydrogen and oxygen sides at less than 0.5atm all the times by employing the proposed Sliding Mode Controller.

2. Dynamic model of a PEM Fuel Cell

The two Models of PEMFC are considered in this work namely, the Stack voltage model and the State space dynamic model. Brief descriptions of these models of PEMFC are presented below.

2.1. Stack Voltage Model of PEMFC

A PEMFC produces the voltage around 0.7v which is not suitable for real time applications. So, PEMFC stack is formed by connecting multiple numbers of single cells in

series by bipolar plates to produce a voltage that is suitable for all applications. Each cell has proton exchange membrane which is sandwiched between two electrodes (anode and cathode) with platinum catalyst. Figure 1 shows the whole operation of PEMFC schematically.

The 99.9% pure, well humidified Hydrogen with stoichiometry of 2 is supplied at the anode with the help of a pressure regulator and purging system. At the same time, an humidified air which has Nitrogen and Oxygen in the ratio of 79:21 with stoichiometry ranges from 2 to 2.5 is supplied through air compressor, air filter and flow controller to the cathode. [17],[18]

The actual fuel cell stack output voltage is decreased from its reversible thermodynamic voltage due to irreversible losses. It can be expressed by the following equation,

$$V_{\text{stack}} = E_{\text{Nernst}} - \eta_{\text{act}} - \eta_{\text{ohm}} - \eta_{\text{conc}} \quad (1)$$

The Nernst equation to represent the reversible thermodynamically predicted stack voltage is,

$$E_{\text{Nernst}} = N \left[V_0 + \left(\frac{RT}{2F} \right) \ln \left(\frac{P_{\text{H}_2} \cdot \sqrt{P_{\text{O}_2}}}{P_{\text{H}_2\text{O}}} \right) \right] \quad (2)$$

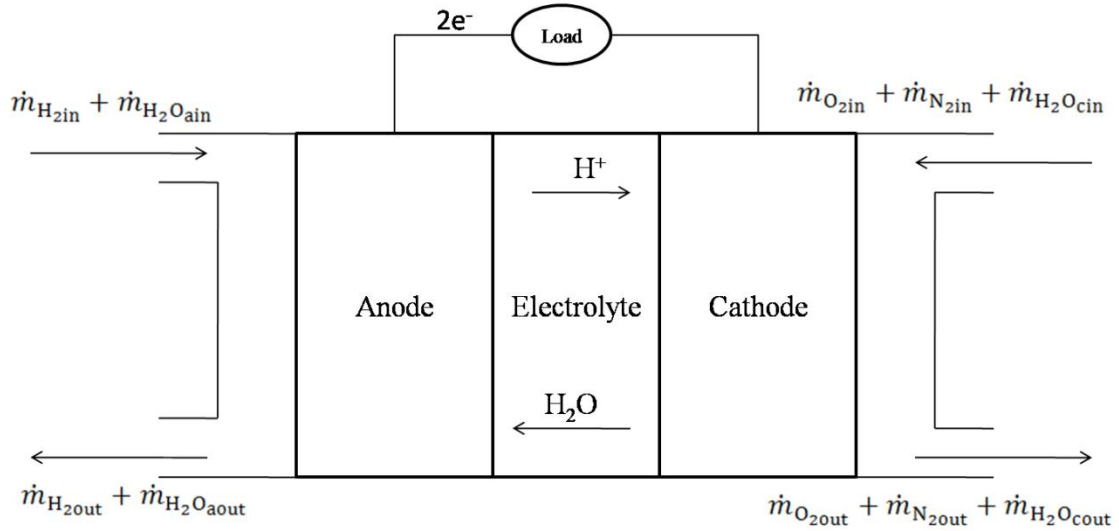


Fig. 1. Schematic diagram of a PEMFC

surface causes reduction in concentration of reactants, can be written as,

$$\eta_{\text{conc}} = N \cdot m \cdot \exp(n \cdot I_f) \quad (5)$$

The activation loss is caused by the sluggishness of electrochemical reaction on the surface of the electrode. Thus the loss in voltage to drive the electrochemical reaction for transferring the electrons to or from the electrode can be described by,

$$\eta_{\text{act}} = N \cdot \frac{RT}{2\alpha F} \cdot \ln \left(\frac{I_f + I_0}{I_0} \right) \quad (3)$$

The ohmic loss due to the resistance to the flow of electrons through the electrodes and their interconnections, as well as the resistance to the flow of ions through the membrane can be expressed by,

$$\eta_{\text{ohm}} = N \cdot I_f \cdot r \quad (4)$$

The mass transport or concentration loss due to the failure of sufficient reactants supply to the electrodes

2.2. State Space Dynamic Model of PEMFC

The following assumptions are made to derive a nonlinear MIMO dynamic model for PEMFC. (1) The Ideal gas law is applied for all gases. (2) The stack temperature is taken as a constant and uniform over the stack. (3) The well humidified reactants are supplied on both sides of the membrane. (4) A pure hydrogen (99.99%) with stoichiometry of 2 and air which is composed of uniformly mixed nitrogen and oxygen in the ratio of 79:21 with stoichiometry ranges from 2 to 2.5 is supplied to the anode and cathode respectively. (5) The reactants is assumed to be humidified by the excess condensed liquid water when those humidity drops below 100%. [17]-[19]

The state space pressure dynamic model of PEMFC is derived by applying ideal gas law and mass conservation principle. The anode dynamic state model the rate of change of partial pressures of hydrogen and water, the cathode dynamic state model has the rate of change of partial pressures of Oxygen, Nitrogen, and water respectively. Whereas the change in partial pressure of reactants and water is balanced by the ideal gas law and the mass conservation principle, the rate of change of partial pressure of each gas is balanced inlet flow rate of reactants minus the reactant's consumption and the outlet flow rate reactants based on ideal gas law and mass conservation principle. The partial pressure derivatives are presented below.

◆Anode Pressure Dynamic model:

The rate of change of partial pressure of hydrogen and water at anode is expressed by the following equations.

$$\frac{dP_{H_2}}{dt} = \frac{RT}{V_a} (\dot{m}_{H_{2in}} - \dot{m}_{H_{2used}} - \dot{m}_{H_{2out}}) \quad (6)$$

$$\frac{dP_{H_2O_a}}{dt} = \frac{RT}{V_a} (\dot{m}_{H_2O_{ain}} - \dot{m}_{H_2O_{aout}} - \dot{m}_{H_2O_{ambr}}) \quad (7)$$

◆Cathode Pressure Dynamic model:

The rate of change of partial pressure of oxygen, nitrogen and water at cathode is expressed by the following equations.

$$\frac{dP_{O_2}}{dt} = \frac{RT}{V_c} (\dot{m}_{O_{2in}} - \dot{m}_{O_{2used}} - \dot{m}_{O_{2out}}) \quad (8)$$

$$\frac{dP_{N_2}}{dt} = \frac{RT}{V_c} (\dot{m}_{N_{2in}} - \dot{m}_{N_{2out}}) \quad (9)$$

$$\frac{dP_{H_2O_c}}{dt} = \frac{RT}{V_c} (\dot{m}_{H_2O_{cin}} - \dot{m}_{H_2O_{cout}} + \dot{m}_{H_2O_{cprod}} + \dot{m}_{H_2O_{ambr}}) \quad (10)$$

Each mole of hydrogen reaction delivers two electrons to the external circuit. Hence, the rate of usage of hydrogen and production of water in terms of stack current are expressed by,

$$\dot{m}_{H_{2used}} = \dot{m}_{H_2O_{cprod}} = \frac{NA}{2F} I_f = a_1 I_f \quad (11)$$

Similarly the rate of oxygen usage is derived; each mole of oxygen transfers four electrons. So, the rate of oxygen reaction is expressed by,

$$\dot{m}_{O_{2used}} = \frac{NA}{4F} I_f = \frac{a_1}{2} I_f \quad (12)$$

The membrane water content is assumed to be a constant ($\lambda m=14$), since the solid polymer membrane is fully humidified. The membrane inlet flow rate of water is written in terms of stack current as follows,

$$\dot{m}_{H_2O_{ambr}} = \frac{1.2684NAI_f}{F} = a_2 I_f \quad (13)$$

Exit flow rate of reactant is calculated from inlet flow rate of reactant minus reactant's usage on both side of stack.

The total anode pressure is expressed by the sum of partial pressure of hydrogen and water.

$$P_a = P_{H_2} + P_{H_2O_a} \quad (14)$$

The cathode pressure is written as the sum of partial pressure of oxygen, nitrogen and added water.

$$P_c = P_{O_2} + P_{N_2} + P_{H_2O_c} \quad (15)$$

State space dynamic equations for rate of change of pressure on the anode side,

$$\frac{dP_{H_2}}{dt} = \frac{RT}{V_a} (\dot{m}_{H_{2in}} - a_1 \cdot I_f - (\dot{m}_{ain} - a_1 \cdot I_f) \cdot \frac{P_{H_2}}{P_a}) \quad (16)$$

$$\frac{dP_{H_2O_a}}{dt} = \frac{RT}{V_a} (\dot{m}_{H_2O_{ain}} - (\dot{m}_{ain} - a_1 \cdot I_f) \cdot \frac{P_{H_2O_a}}{P_a} - a_2 I_f) \quad (17)$$

State space dynamic equations for rate of change of pressure on the cathode side,

$$\frac{dP_{O_2}}{dt} = \frac{RT}{V_c} (\dot{m}_{O_{2in}} - \frac{a_1}{2} I_f - (\dot{m}_{cin} - \frac{a_1}{2} \cdot I_f) \cdot \frac{P_{O_2}}{P_c}) \quad (18)$$

$$\frac{dP_{H_2O_c}}{dt} = \frac{RT}{V_c} (\dot{m}_{H_2O_{cin}} + a_1 I_f - (\dot{m}_{cin} + a_1 \cdot I_f + a_2 \cdot I_f) \cdot \frac{P_{H_2O_c}}{P_c} + a_2 \cdot I_f) \quad (19)$$

$$\frac{dP_{N_2}}{dt} = \frac{RT}{V_c} (\dot{m}_{N_{2in}} - \dot{m}_{cin} \cdot \frac{P_{N_2}}{P_c}) \quad (20)$$

State space dynamic equations for rate of change of pressure on the anode side,

$$\frac{dP_{H_2}}{dt} = \frac{RT}{V_a} (\dot{m}_{H_{2in}} - a_1 \cdot I_f - (\dot{m}_{ain} - a_1 \cdot I_f) \cdot \frac{P_{H_2}}{P_a}) \quad (21)$$

$$\frac{dP_{H_2O_a}}{dt} = \frac{RT}{V_a} (\dot{m}_{H_2O_{ain}} - (\dot{m}_{ain} - a_1 \cdot I_f) \cdot \frac{P_{H_2O_a}}{P_a} - a_2 I_f) \quad (22)$$

State space dynamic equations for rate of change of pressure on the cathode side,

$$\frac{dP_{O_2}}{dt} = \frac{RT}{V_c} (\dot{m}_{O_{2in}} - \frac{a_1}{2} I_f - (\dot{m}_{cin} - \frac{a_1}{2} \cdot I_f) \cdot \frac{P_{O_2}}{P_c}) \quad (23)$$

$$\frac{dP_{H_2O_c}}{dt} = \frac{RT}{V_c} (\dot{m}_{H_2O_{cin}} + a_1 I_f - (\dot{m}_{cin} + a_1 \cdot I_f + a_2 \cdot I_f) \cdot \frac{P_{H_2O_c}}{P_c} + a_2 \cdot I_f) \quad (24)$$

$$\frac{dP_{N_2}}{dt} = \frac{RT}{V_c} (\dot{m}_{N_{2in}} - \dot{m}_{cin} \cdot \frac{P_{N_2}}{P_c}) \quad (25)$$

The mole fractions of the Hydrogen (n_{H_2}) is 0.99. Hence, the inlet flow rate of hydrogen is expressed as,

$$\dot{m}_{H_{2in}} = n_{H_2} \cdot \dot{m}_{ain} \quad (26)$$

The mole fractions of the Oxygen (n_{O_2}) and Nitrogen (n_{N_2}) in air are 0.21 and 0.79 respectively. Hence the inlet flow rates of oxygen and nitrogen is written as,

$$\dot{m}_{O_{2in}} = n_{O_2} \cdot \dot{m}_{cin} \quad (27)$$

$$\dot{m}_{N_{2in}} = n_{N_2} \cdot \dot{m}_{cin} \quad (28)$$

The water inlet flow rate at the anode and the cathode are expressed as follows;

$$\dot{m}_{H_2O_{ain}} = \frac{\phi_a \cdot P_v}{P_a - \phi_a \cdot P_v} \cdot \dot{m}_{ain} \quad (29)$$

$$\dot{m}_{H_2O_{cin}} = \frac{\phi_c \cdot P_v}{P_c - \phi_c \cdot P_v} \cdot \dot{m}_{cin} \quad (30)$$

Moreover, the reactants' inlet flow rates are calculated from the product of controller output, conversion factor and stoichiometry ratio of the reactants on both side of the membrane.

$$\dot{m}_{ain} = u_1 \cdot c_a \cdot \lambda_{H_2} \quad (31)$$

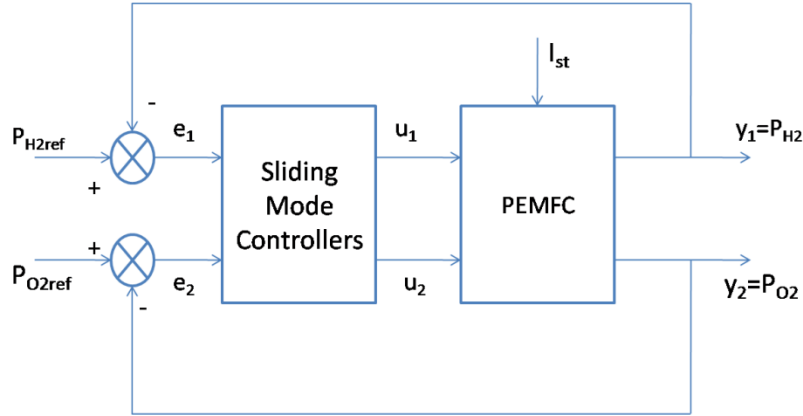


Fig 2. Proposed Sliding Mode Controllers for pressure regulation of PEMFC

The Sliding Mode Controller which is shown in Figure 2 is proposed to maintain the Partial pressure of Hydrogen at the anode and Oxygen at the cathode for PEMFC system under dynamic load changing condition through the control of mass flow rate of Hydrogen and Oxygen at anode and cathode respectively. The proposed controller is robust under dynamic load variations. Thus the SMCs follow the set points of input reactants' pressure and also keep the pressure difference between two sides as very small. Moreover, the SMCs avoid the reactants' starvation by supplying the enough reactants to both side of the PEMFC.

Let a nonlinear MIMO system with a disturbance can be described in continuous form by the following equation,

$$\dot{X} = f(X, t) + \sum_{i=1}^m g_i(X, t) \cdot u_i + p(X, t) \cdot d, \quad i = 1, 2, \dots, m \quad (33)$$

$$y_i = h_i(X, t), \quad i = 1, 2, \dots, m \quad (34)$$

$$\dot{m}_{cin} = u_2 \cdot c_c \cdot \lambda_{air} \quad (32)$$

2.3. Sliding Mode Control for PEMFC

Sliding Mode Controller (SMC) is more attractive for its simplicity and robustness to disturbances and parameter variations. Hence, it is widely used in uncertain system or system with lack of information available for modeling. [20] The control law of SMC is designed to attract the system trajectory to sliding surface and once the trajectory reaches it, keep the trajectory on the sliding surface subsequently. Thus this motion of system trajectory is called as sliding motion. The control action of the SMC is working in two distinct phase of motion such as 'reaching phase' in which control law attracts the system trajectories to reach the sliding surface from any initial condition and 'sliding mode phase' that keeps the system trajectories to remain in sliding surface for the rest of the period. [21]

Where, $x \in R^n$ are the system state variables, $u \in R^m$ are the control variables and $y = R_p$ are the output variables. And also f and g are n -dimensional nonlinear vectors, h is the m -dimensional output vectors, d is the disturbance and p is the vector field related to the disturbance.

Hence the nonlinear dynamic MIMO state space model for PEMFC can be derived as follows,

$$\dot{X} = f(X, t) + g_1(X, t) \cdot u_1 + g_2(X, t) \cdot u_2 + p(X, t) \cdot d \quad (35)$$

$$\begin{bmatrix} y_1 \\ y_2 \end{bmatrix} = \begin{bmatrix} x_1 \\ x_2 \end{bmatrix} = \begin{bmatrix} h_1(x) \\ h_2(x) \end{bmatrix} \quad (36)$$

The state variables, control variables, output variables and disturbance of PEMFC system can be expressed as,

◆State Variables:

$$[x_1 x_2 x_3 x_4 x_5] = [P_{H_2} P_{H_2O_a} P_{O_2} P_{N_2} P_{H_2O_c}] \quad (37)$$

◆Control Variables:

$$[u_1 u_2] = [u_a u_b] \quad (38)$$

◆Output Variables:

$$[y_1 y_2] = [P_{H_2} P_{O_2}] \quad (39)$$

◆Disturbance:

$$d = I_{st} \quad (40)$$

A control law is developed to keep the reactants' partial pressures at set points by nullifying the errors (e_1, e_2) which is the difference between the measured values of partial pressure of the reactants (P_{H_2}, P_{O_2}) and reference values (P_{H_2ref}, P_{O_2ref}). The Figure3 shows the schematic diagram of proposed sliding mode control strategy. The sliding manifolds in which the errors are zero can be expressed mathematically as follows;

$$S(x, t) = \left(c_1 \frac{d}{dt} + c_2 \right)^{n-1} e \quad (41)$$

Substituting $n=2$ gives

$$S(x, t) = \left(c_1 \frac{de}{dt} + c_2 e \right) \quad (42)$$

The control law is derived from the Lyapunov function where sliding surface is considered as $S(x,t)=0$ and $\frac{dS(x,t)}{dt} \leq -\eta$. Hence, it can be expressed as,

$$U = -M \cdot \text{sat}(S(x,t)) \quad (43)$$

Where, constants c_1, c_2, η and $M > 0$

To avoid the chattering phenomenon in Sliding Mode control, the 'saturation' function is employed here instead of 'signum' function.

3. Simulation model of PEMFC and proposed Sliding Mode Control

The developed mathematical models of PEMFC presented in section 2.1 and 2.2 and the Sliding Mode controller presented in section 2.3 are built as simulation models in MATLAB-SIMULINK. The snapshots of the developed simulation models are presented below from figure 4 to 6.

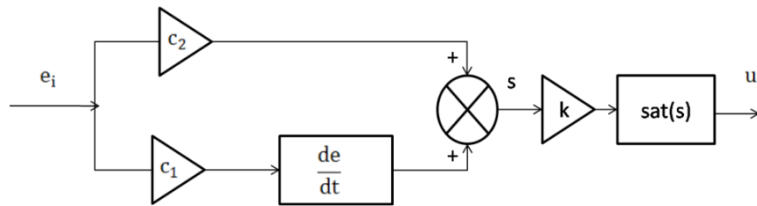


Fig 3. Schematic diagram of Sliding Mode Controller

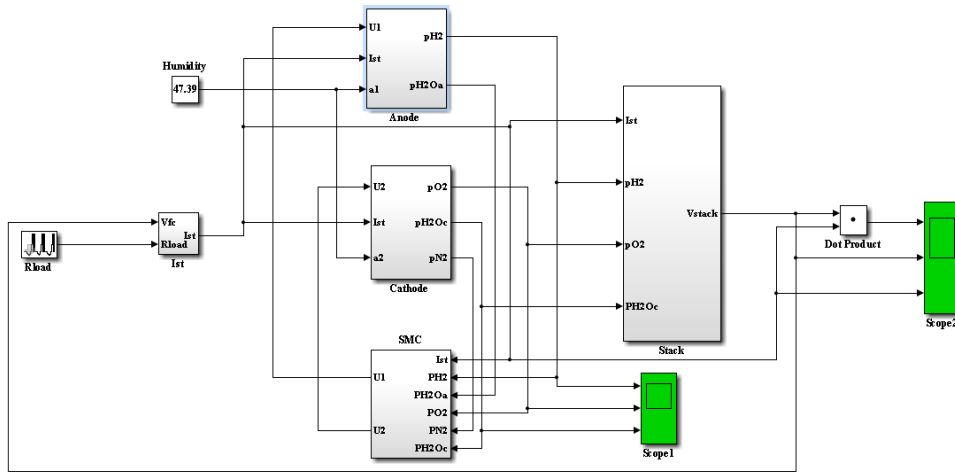


Fig 4. PEMFC Model

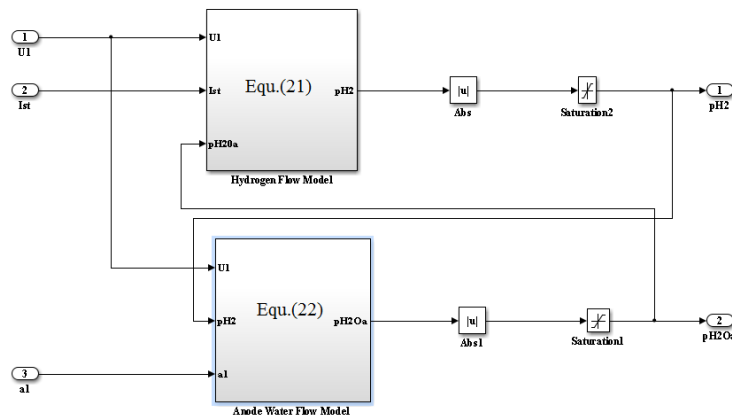


Fig 5. Anode Model

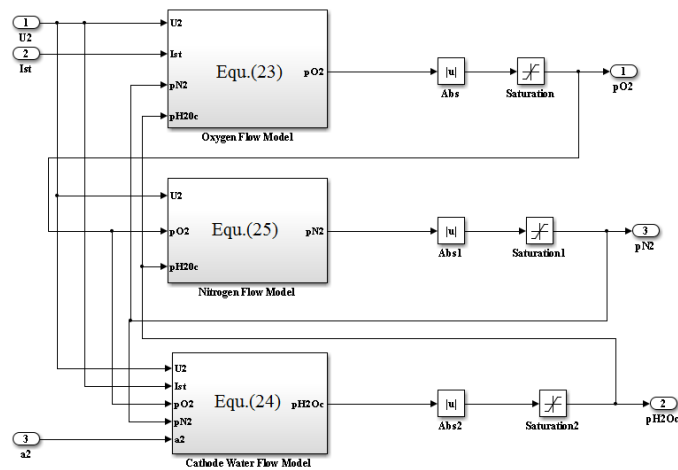


Fig 6. Cathode Model

4. Results and discussion

The PEMFC Stack voltage, State space dynamic anode and cathode model along with Sliding Mode Controller have been developed in MATLAB-SIMULINK, version 8.1 (R2013a). In order to keep the partial pressure of Hydrogen at anode and Oxygen at cathode side at set-points 3atm, 4atm and 5atm under dynamic load changing condition, two Sliding Mode Controllers are employed on both sides of the PEMFC.

The large deviation of reactant pressure from the set-point will rush the membrane at high pressure side and also lead to severe damage to membrane and thereby shortening the life of PEMFC. Hence, it is very much essential to ensure the difference between these pressures are maintained at the smallest possible level and also keep the constant reactant pressure on both sides of the Polymer Electrolyte Membrane. This helps to improve the performance and life of PEMFC.

The simulation results of proposed Sliding Mode Controller, for dynamic load changing profile with the step change in set-point from 3atm to 5atm, have been compared with the results of PI controller and presented graphically through figures 8 to figure 13.

The dynamic load profile for the simulation experiments is generated using a timer in the Simulink. The dynamic load profile for assessing the performance of PEMFC is shown in Figure 7.

When the dynamic load change is applied, the Fuel Cell current, Stack Voltage and Power Demand vary between 6.5 and 165.5A, 28.2 and 33.1V and 0.22 and 4.49KW respectively. These are presented in Figure 8, 9 and 10 respectively. The difference between the response of proposed SMC and conventional PI controller is shown in these figures with a portion zoomed.

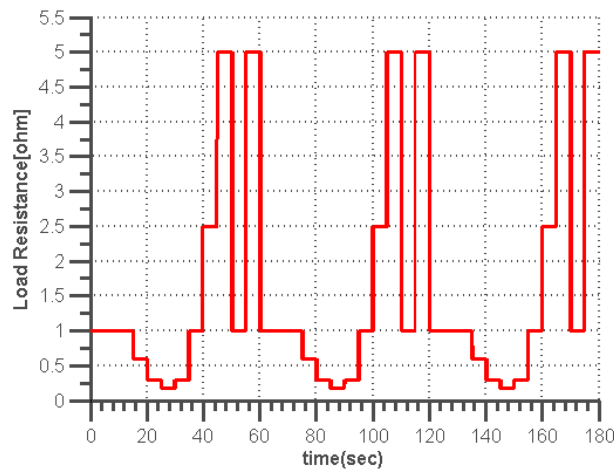


Fig 7. Dynamic load profile

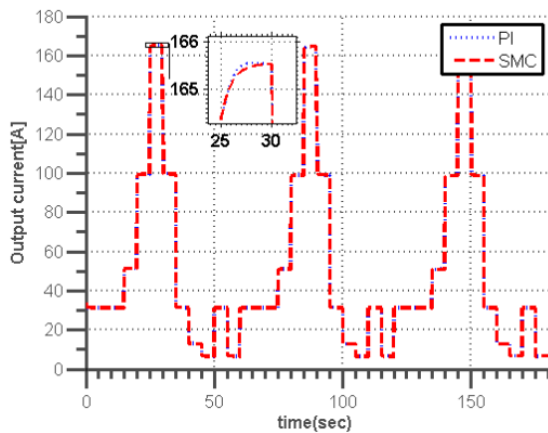


Fig 8. PEMFC output current

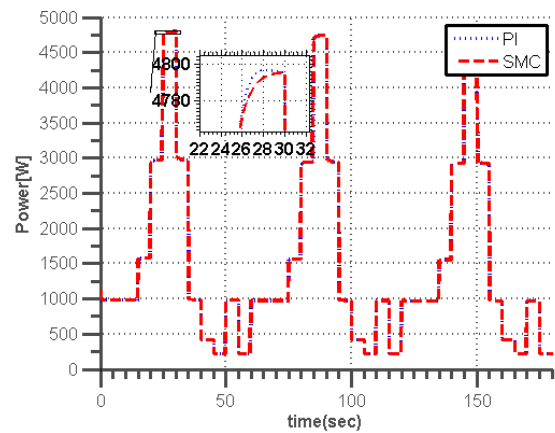


Fig 9. PEMFC power output

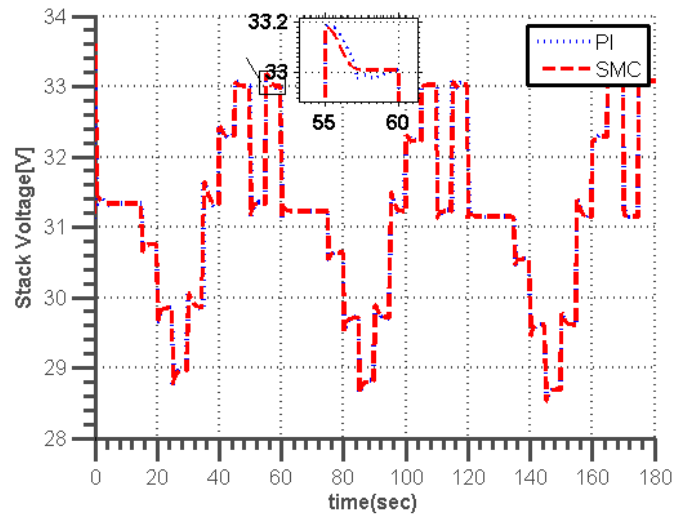


Fig 10. PEMFC stack voltage

The hydrogen flow rate of PEMFC under Sliding Mode Control varies between 0.176 and 4.4 SLPM, while its value changes between 0.133 and 4.49 SLPM under PI control. The response of Sliding Mode Control is very fast when compared to the PI control except for the load changing condition which is shown in Figure 11. At the cathode side, the Oxygen flow rate varies in the range of 0.86 to 13.68 SLPM and 0.35 to 13.23 SLPM for Sliding Mode Control and PI control respectively.

As seen in Figure 11, PEMFC with Sliding Mode Control regulates Oxygen flow rate very smoothly and quickly during dynamic load change. Since oxygen flow rate is more sensitive than hydrogen flow rate under dynamic load changing condition, its variation is larger when compared with the hydrogen flow rate.

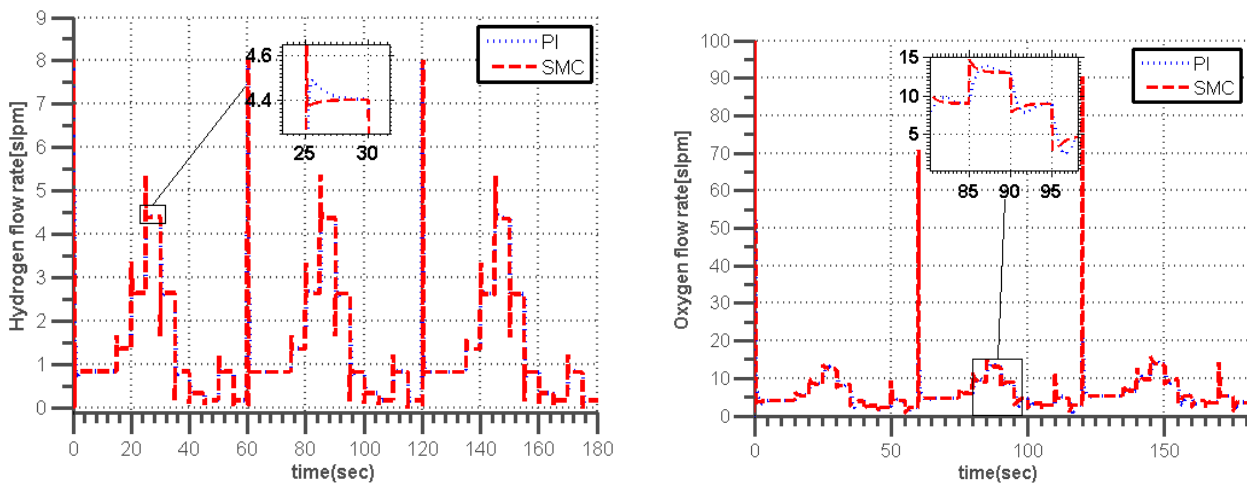


Fig 11. Mass flow rates of Hydrogen at anode and Oxygen at cathode

Further, it is evident that the result of maximum deviation of hydrogen pressure from reference point is just 0.04 under Sliding Mode Control against 0.13 deviation of PI control. The proposed controller for oxygen pressure

regulation is much better than the PI control. It produces less than 0.001 pressure difference while it is 0.896atm by the conventional PI control. These facts can be seen from the figure 12.

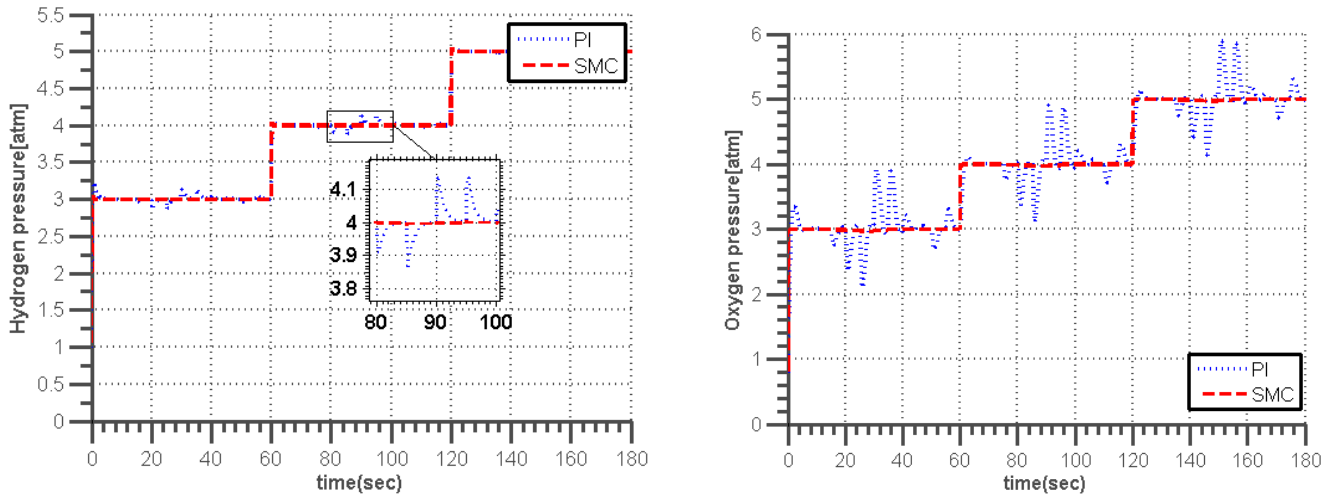


Fig 12. Partial pressures of Hydrogen and Oxygen for step change in set point from 3atm to 5atm

Pressure difference between the reactants is another factor to be seriously concerned. The proposed Sliding Mode Control keeps the pressure difference between reactants below 0.05atm whereas conventional control

maintains 0.89atm pressure deviation. This can be seen in Figure 11. Hence, it is evident that the proposed controller keeps tracking the reference reactants pressure and avoids large pressure difference between reactants on both sides.

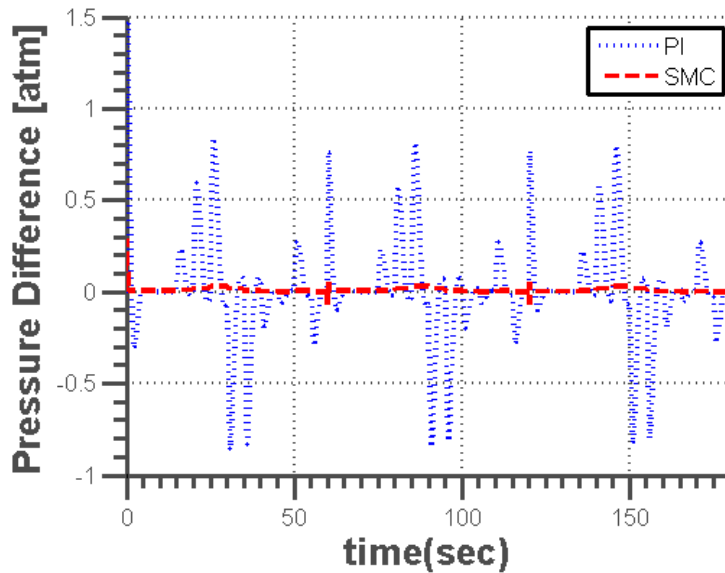


Fig13. Pressure difference between reactants at anode and cathode

In addition to the graphical presentation of simulation results given above, the extracted time response parameters from these results are tabulated in Table 1. The error criteria IAE, ISE, ITAE and ITSE have been evaluated for both the

controllers. Again, the values of these error parameters also show that the proposed Sliding Mode Controller performs much better than the conventional PI controller.

TABLE 1: COMPARISON OF ERRORS EXHIBITED BY SLIDING MODE AND PI CONTROLLERS

CONTROLLER	PH ₂				PO ₂			
	IAE	ISE	ITAE	ITSE	IAE	ISE	ITAE	ITSE
PI	3.328	0.812	248.389	24.58	29.64	15.648	2558.71	1233.757
SMC	0.736	0.617	33.482	10.538	2.433	0.731	175.526	12.240

CONCLUSION

This study reveals that the proposed Sliding Mode Controller protects the membrane from severe damage which is caused by large pressure deviation of reactants to prolong the life of the stack. A MIMO non-linear control oriented dynamic model is developed and the Sliding Mode Controllers are used for the regulation of hydrogen pressure at anode side and oxygen pressure at the cathode by controlling the mass flow rate of the reactants. The results prove that the proposed Sliding Mode Controller performs much better than the conventional PI controller, under dynamic load change conditions for various set-points.

REFERENCES

[1] Wang, Y., Chen, K., Mishler, J., Cho, S. and Adroher, X (2011). A review of polymer electrolyte membrane fuel cells: Technology, applications, and needs on fundamental research. *Applied Energy*, 88(4): 981-1007.

[2] Karnik, AY, Sun, J, Stefanopoulou, AG & Buckland, JH 2009, 'Humidity and pressure regulation in a PEM Fuel Cell using a Gain-scheduled static feedback controller', *IEEE Transaction on control system technology*, vol. 17, no. 2, pp. 283-297.

[3] Pukrushpan, J.T., Stefanopoulou, A.G., and Peng, H (2004). Control of fuel cell breathing. *IEEE Control Systems Magazine*, 24(2), 30-46.

[4] Pukrushpan, J., Stefanopoulou, A., Varigonda, S., Eborn, J., and Haugstetter, C (2006). Control-oriented model of fuel processor for hydrogen generation in fuel cell applications, *Control Engineering Practice*, 14(3): 277-293.

[5] Rodatz, P., Paganelli, G., and Guzzella, L (2003). Optimization air supply control of a PEM Fuel Cell system, In: *Proceedings of the 2003 American control conference*.

[6] Pukrushpan, J.T., Stefanopoulou, A.G., and Peng, H (2004). Control of fuel cell power systems: Principles, modeling and analysis and feedback design, In: *Advances in industrial control*. Berlin: Springer.

[7] Markus Ozbek, Shen Wang, Matthias Marx, Dirk Soffker (2013). Modeling and control of a PEM fuel cell system: A practical study based on experimental defined component behavior, *Journal of Process Control*, 23(3): 282-293.

[8] Shen C, Cao GY, Zhu XJ and Sun XJ (2002). Nonlinear modeling and adaptive fuzzy control of MCFC stack, *Journal of Process Control*, 12(8): 831-839.

[9] Schumacher JO, Gemmar P, Denne M, Zedda M, and Stueber M (2004). Control of miniature proton exchange membrane, fuel cells based on fuzzy logic, *Journal of Power Sources*, 129(2): 143-151.

[10] Iwan LC, Stengel RF (2001). The application of neural networks to fuel processors for fuel-cell vehicles, *IEEE Transactions on Vehicular Technology*, 50(1): 125-143.

[11] Almeida, P.E.M., and Simoes, M.G. (2005). Neural optimal control of PEM fuel cells with parametric CMAC networks. *IEEE Transactions on Industry Applications*, 41(1): 237-245.

[12] Hamed Beirami, Ali Zargar Shabestari and Mohammad Mahdi Zerafat (2015). Optimal PID plus fuzzy controller design for a PEM fuel cell air feed system using the self-adaptive differential evolution algorithm, *International Journal of Hydrogen Energy*, 40(30): 9422-9434.

[13] Gruber, J.K, Doll, M and Bordons, C (2009). Design and experimental validation of a constrained MPC for the air feed of a fuel cell, *Control Engineering Practice*, 17: 874-885.

[14] Alicia Arce, Alejandro J. del Real, Carlos Bordons and Daniel R. Ramirez (2010). Real-Time Implementation of a Constrained MPC for Efficient Airflow Control in a PEM Fuel Cell, *IEEE transactions on industrial electronics*, 57(6): 1892-1905.

[15] Varigonda S and Kamat M (2006). Control of stationary and transportation fuel cell systems: Progress and opportunities, *Computers and Chemical Engineering*, 30(10-12): 1735-1748.

[16] Larminie, J & Dicks, A 2000, 'Fuel cell systems explained', United Kingdom, John Wiley & Sons.

[17] Gou B, Na W and Diang B (2010) *Fuel Cells: Modelling, Control, and Applications*. Boca Raton: CRC Press.

[18] Na W and Gou B (2007). Exact linearization based nonlinear control of PEM Fuel Cells, *Proceedings of IEEE Power Engineering Society General Meeting, FL, USA, 24-28 June 2007*, pp. 1-6.

[19] Kunusch C, Puleston P and Mayosky M (2012). *Sliding-Mode Control of PEM Fuel Cells*. Springer-Verlag London.

[20] Boopathi A and Abudhahir A (2016). Design of Grey-Verhulst Sliding Mode Controller for Antilock Braking System, *International Journal of Control, Automation, and Systems*, 14(3): 763-772.

[21] Boopathi A and Abudhahir A (2016). Adaptive Fuzzy Sliding Mode Controller for wheel slip control in Antilock Braking System, *Journal of Engineering Research*, 4(2): 132-150.

NOMENCLATURE

E_{Nernst}	Nernst voltage	Volts
η_{act}	Activation loss	Volts
η_{ohm}	Ohmic loss	Volts
η_{conc}	concentration loss	Volts
N	Number of fuel cells in the stack	--
V_0	Open cell voltage	Volts
R	Universal gas constant	J/mol-K
T	Temperature of the stack	K
F	Faraday's constant	C/mol
$P_{H_2}, P_{H_2O_a}$	Partial pressure of Hydrogen and Water at anode	Atm

P_{O_2}, P_{N_2} and $P_{H_2O_c}$	Partial pressure of Oxygen , Nitrogen and Water at cathode respectively	Atm
P_v, P_a and P_c	saturated vapour pressure, total anode and cathode pressures	Atm
r	Area specific resistance	$K\Omega\text{-cm}^2$
m, n	Coefficients of mass transfer voltage	--
I_f, I_0, I_n	Output, Exchange and Internal Current Densities respectively	A/cm^2
A	Cell active area	cm^2
V_a, V_c	Volume of anode and cathode respectively	m^3
ϕ_a and ϕ_c	Relative humidities on the anode and the cathode sides	--
I_{st}	Stack Current	A
c_a, c_a	Conversion factor	--
u_a, u_c	Control variables	--
a_1, a_2	Constants	--
$\dot{m}_{a_{in}}, \dot{m}_{c_{in}}$	Total Mass flow rate at anode and cathode respectively	mol/s
$\dot{m}_{H_2in}, \dot{m}_{H_2out}$	Mass flow rate of hydrogen at anode Inlet and outlet respectively	mol/s

$\dot{m}_{H_2O_{ain}}, \dot{m}_{H_2O_{aout}}$	Mass flow rate of water at anode Inlet and outlet respectively	mol/s
$\dot{m}_{H_2O_{cin}}, \dot{m}_{H_2O_{cout}}$	Mass flow rate of water at cathode Inlet and outlet respectively	mol/s
$\dot{m}_{N_2in}, \dot{m}_{N_2out}$	Mass flow rate of nitrogen at cathode Inlet and outlet respectively	mol/s
$\dot{m}_{O_2in}, \dot{m}_{O_2out}$	Mass flow rate of oxygen at cathode Inlet and outlet respectively	mol/s